HHS Public Access

Author manuscript

Anal Chem. Author manuscript; available in PMC 2024 July 27.

Published in final edited form as:

Anal Chem. 2024 April 23; 96(16): 6347–6355. doi:10.1021/acs.analchem.4c00030.

In-Membrane Enrichment and Peptic Digestion to Facilitate Analysis of Monoclonal Antibody Glycosylation

Junyan Yang[1], **Raluca Ostafe**[2], **Merlin L. Bruening**[1,3,*]

[1]Department of Chemical and Biomolecular Engineering, University of Notre Dame, Notre Dame, IN 46556, United States

[2]Molecular Evolution, Protein Engineering and Production Facility; Purdue Institute for Inflammation, Immunology and Infection Diseases, Purdue University, West Lafayette, IN 47907, United States

[3]Department of Chemistry and Biochemistry, University of Notre Dame, Notre Dame, IN 46556, United States

Abstract

The number of therapeutic monoclonal antibodies (mAbs) is growing rapidly due to their widespread use for treating various diseases and health conditions. Assessing the glycosylation profile of mAbs during production is essential to ensure their safety and efficacy. This research aims to rapidly isolate and digest mAbs for LC-MS/MS identification of glycans and monitoring of glycosylation patterns, potentially during manufacturing. Immobilization of an Fc region-specific ligand, oFc20, in a porous membrane enables enrichment of mAbs from cell culture supernatant and efficient elution with an acidic solution. Subsequent digestion of the mAb eluate occurs in a pepsin-modified membrane within 5 min. The procedure does not require alkylation and desalting, greatly shortening sample preparation time. Subsequent LC-MS/MS analysis identified eleven major mAb N-glycan proteoforms and assessed the relative peak areas of the glycosylated peptides. This approach is suitable for glycosylation profiling of various human IgG mAbs, including biosimilars and different IgG subclasses. The total time required for this workflow is less than 2 hours, whereas the conventional enzymatic release and labelling of glycans can take much longer. Thus, the integrated membranes are suitable for facilitating analysis of mAb glycosylation patterns.

Graphical Abstract

[*]**Corresponding Author Merlin L. Bruening** – Department of Chemical and, Biomolecular Engineering, University of Notre Dame, Notre, Dame, Indiana 46556, United States; mbruenin@nd.edu.

Author Contributions

The manuscript was written through contributions of all authors. All authors have given approval to the final version of the manuscript.

ASSOCIATED CONTENT

Supporting Information

The Supporting Information is available free of charge on the ACS Publications website.

Data analysis methods, comparison with Protein A spin columns, list of glycopeptides and theoretical monoisotopic masses or m/z values, selected XICs, MS1 and MS2 spectra, Trastuzumab degradation results, and glycan compositions of other Human IgG mAbs. (PDF).

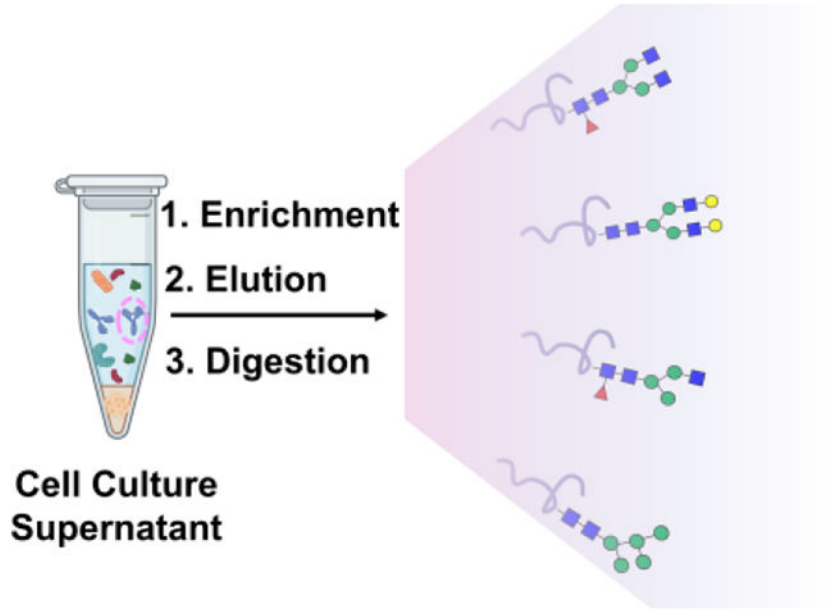

INTRODUCTION

This paper describes a convenient and broadly applicable method for assessment of N-glycan profiles on human IgG monoclonal antibodies (mAbs). The process includes selective enrichment of mAbs in an affinity membrane, elution in 3% formic acid (FA), and fast proteolysis in a pepsin-containing membrane to remarkably shorten sample preparation time and avoid the requirements of alkylation and desalting. LC-MS/MS identifies various mAb proteoforms and gives an estimate of the relative peak areas of N-glycosylated peptides. This approach could enable monitoring of mAb glycan compositions during fermentation.

mAbs serve as highly effective biotherapeutics for multiple diseases,[1–3] and control and assessment of mAb compositions and post-translational modifications (PTMs) are critical during mAb production.[4, 5] Glycosylation is one of the most important mAb critical quality attributes that should be monitored.[6] The wide range of glycan proteoforms[7] possess different pharmacological properties, including antibody-dependent cellular cytotoxicity (ADCC),[8] complement-dependent cytotoxicity, immunogenicity and pharmacokinetics (PK).[9] For example, afucosylated IgG mAbs show higher ADCC through increased IgG-FcγRIIIa affinity.[10] Different expression systems may greatly impact glycan formation. For example, plants, insects, or yeast[6, 11] utilize different glycans compared to mammalian systems, which can lead to immunogenic events. Furthermore, throughout fermentation and scaling up of mAb synthesis, the glycosylation patterns of mAbs may depend on factors such as the composition of the growth media and cell densities.[12] These changes can yield mAbs with distinct pharmacokinetic properties when compared to those tested in smaller-scale experiments or previous batches. Regular monitoring of glycosylation patterns during fermentation can facilitate early intervention to maintain the quality of the mAbs.[13]

Glycans are also attractive targets for modifications.[14–16] Researchers explored using N-glycans to create antibody-drug conjugates (ADCs). Zhu et al. employed galactosidase to generate a uniform G0F glycan and then derivatized the N-acetylglucosamine to link the cytotoxic drug auristatin F to the mAb.[17] Zhou et al. linked monomethylauristatin E to oxidized sialic acids of glycans to produce an ADC.[18] Thus, understanding the glycosylation pattern of mAbs is vital for mAb function and derivatization.

The most common method for analyzing N-glycan compositions on mAbs includes cleavage of glycans from proteins using peptide N-glycosidase F (PNGase F) followed by fluorescently labelling released glycans.[19] The labelled glycans are analyzed by high-performance liquid chromatography with fluorescence detection. However, the glycan release requires mAb incubation with PNGase F for hours.[20] Szigeti et al. reported a method to rapidly release N-glycans from proteins using a microcolumn containing immobilized PNGase F.[21] Although the use of the microcolumn shortens the lysis time significantly, chemically labelling cleaved glycans with 2-aminobenzamide (2-AB) still takes hours, sometimes even days to finish. Agilent advertised a new approach where PNGase F digestion is as short as 5 min, and 2-AB labelling can be achieved within 2 hours.[22] However, the enzymatically released glycan approaches do not reveal the amount of aglycosylated protein or identify the glycosylation site.

Alternative methods for glycan profiling usually involve either intact protein analysis[23] or mAb digestion through in-solution trypsin proteolysis[24] followed by mass spectrometry analysis.[25, 26] In intact protein methods, only highly abundant glycans are observable.[27] Proteolysis along with the accompanying reduction, alkylation, and desalting can require hours to days.[28] Such methods are not ideal for rapid glycan analysis of mAbs during fermentation. Yang et al. proposed a workflow where mAb tryptic digestion occurs in an environment containing 80% acetonitrile. The resulting digest is lyophilized and then resuspended prior to analysis by matrix-assisted laser desorption/ionization-time of flight mass spectrometry (MALDI-TOF-MS).[29] Although the trypsin digestion time is shorter than conventional conditions, the assay turnaround time is still around 1 hour. The digested product also requires desalting and enrichment prior to analysis, further extending its sample preparation time. Thus, a high-throughput workflow with short turnaround time is in high-demand to profile N-glycan compositions during the production of mAbs.

This work aims to develop methods for rapidly isolating and digesting proteins to expedite LC-MS/MS assessment of glycosylation patterns when monitoring continuity in glycan proteoform expression. In this vein, membranes serve as a useful tool for rapid bioprocessing, including polishing,[30] protein purification[31] and clarification. Our group developed modified membranes for applications ranging from separation of biomolecules[32–34] to controlled proteolysis.[35, 36] Short diffusion times allow rapid sorption of analytes in the membranes. Proteases immobilized in membranes efficiently digest proteins in seconds due to the high local enzyme density and small diffusion distances.[37]

Our prior work focused on using standalone membrane devices for either protein isolation and detection or protein digestion before LC-MS analysis. This work combines two membranes; one selectively enriches mAbs from cell culture supernatant, while the other

rapidly digests mAbs eluted from the former membrane. oFc20 peptide is a double cyclic peptide that has strong affinity towards the Fc region of human IgGs.[38, 39] Protein A is an industrial staple for antibody purification. However, the oFc20-human IgG complex shows a dissociation constant (K_D) of 2.5 nM,[38] even lower than for the Protein A-human IgG complex (K_D = 35 nM).[40] Thus, functionalization of membranes with oFc20 peptide enables rapid separation of mAbs from host cell proteins and other impurities in cell culture supernatant.[39] (Unlike human serum, the mAb should be the only IgG in the fermentation system.)

Using a pepsin-functionalized membrane, controlled proteolysis of eluted mAbs readily generates glycopeptides for assessment by LC-MS. Compared to established methods, our approach integrates two essential parts of N-glycan analysis for mAbs, separation and enzymatic digestion, whereas others only provide one part of the solution. Meanwhile, the turnaround time of this work, from mAb enrichment to final data acquisition by LC-MS is around 2 hours, and half of the time is for LC-MS. The sample processing is significantly shorter than conventional methods and could aid in the optimization or monitoring of mAb production in short times.

EXPERIMENTAL SECTION

Materials.

Glass-fiber membranes (A/C Glass Fiber 1 μm pores, 25 mm diameter, 254 μm thickness) and LoProdyne nylon membranes (1 μm pores, 25 mm diameter, 110 μm thickness) were acquired from Pall Corporation. Sodium phosphate dibasic heptahydrate, sodium phosphate monobasic monohydrate, sodium chloride, sodium hydroxide, polyethylenimine (PEI, branched, M_W = 25 kDa), poly(acrylic acid) (PAA, average M_W ~250 kDa, 35% aqueous solution), poly(sodium 4-styrenesulfonate) (PSS, M_W ~ 70 kDa), pepsin (from porcine gastric mucosa), trypsin (from bovine pancreas, TPCK treated), 1,4-dithiothreitol, iodoacetamide, N-hydroxysuccinimide (NHS), tris(2-carboxyethyl)phosphine hydrochloride (TCEP·HCl), and sodium dodecyl sulfate (SDS) were purchased from Sigma-Aldrich. N-(3-dimethylaminopropyl)-N’-ethylcarbodiimide hydrochloride (EDC), hydrochloric acid, Pierce IgG elution buffer, LC-MS grade formic acid (FA), acetonitrile (ACN), sodium carbonate, sodium bicarbonate and 3.5K MWCO dialysis devices were acquired from ThermoFisher Scientific. Protein A HP spintrap columns were purchased from Cytiva Life Sciences. Fc20 peptide (amino acid sequence: KGSGSCDCAWHLGELVWCTC) in reduced form was synthesized by Genscript with a purity of 97.5%. Trastuzumab (Herceptin from Genentech; Ogivri from Mylan; Kanjinti from Amgen), Bevacizumab (Avastin, Genentech), Rituximab (Rituxan, Genentech), Panitumumab (Vectibix, Amgen) and Nivolumab (Opdivo, Bristol Myers Squibb) were stored in their formulation buffers at −20 °C. Ab3022-containing or blank CHO cell culture supernatant was prepared as described previously.[39] Solutions were prepared using analytical grade chemicals and deionized (DI) water (Milli-Q Type I, 18.2 MΩ·cm).

Immobilization of Pepsin in a 2-cm Diameter Nylon Membrane.

Functionalization of membranes with pepsin occurred following a literature procedure.[41] A 25-mm diameter LoProdyne nylon membrane was cleaned in UV/O_3 for 10 min (Jelight, Model 18 UVO-cleaner) before inserting the membrane into a customized membrane holder[42] (an O-ring reduces its exposed diameter to 2 cm). Ten mL of 20 mM PSS solution (repeating unit concentration, containing 500 mM NaCl, pH 2.3) was circulated through the membrane for 20 min (the flow rate was 1 mL/min unless otherwise noted) before passing 10 mL of DI water and 10 mL of 5% (v/v) FA in water through the membrane. Subsequently, 1 mL of 2 mg/mL pepsin solution (dissolved in 5% FA) was circulated through the membrane for 1 hour before passage of 15 mL of 5% FA. The load, permeate and wash solutions were collected for pepsin analysis (using intrinsic tryptophan fluorescence) to determine the amount of immobilized pepsin.

Immobilization of oxidized Fc20 or Protein A in Glass-Fiber Membranes.

Two mg of Fc20 peptide was dissolved in 2 mL of 20 mM phosphate buffer (containing 150 mM NaCl, pH 7.4, Buffer A) before the pH of the solution was adjusted to 9.0 using 1 M NaOH. The oxidized Fc20 peptide (oFc20) was generated by incubating the Fc20 peptide solution at room temperature overnight with the cap left ajar to allow mild oxidation. Using MALDI-TOF-MS, we previously confirmed that the oFc20 peptide contains two disulfide bonds.[39]

We reported the procedure for immobilizing oFc20 in a glass-fiber membrane.[39] Two PEI/PAA bilayers were deposited before activating the -COOH groups of PAA films by circulating 5 mL of a 0.1 M EDC/NHS (equimolar) solution through the membrane at 1 mL/min. Subsequently, 1 mL of 1 mg/mL oFc20 peptide solution was circulated through the membrane for 1 hour to allow covalent immobilization of oFc20. Finally, 5 mL of a solution containing 10 mM Na_2CO_3 and 90 mM $NaHCO_3$ (pH 9.0, Buffer B) was circulated through the membrane overnight to hydrolyze excess NHS esters. Protein A immobilization in membranes followed the same steps, except 1 mL of 1 mg/mL Protein A (in Buffer A) was circulated, and no Buffer B circulation was performed.

Binding and Elution of Trastuzumab in Ligand-Modified Membranes.

After overnight Buffer B circulation, 10 mL of DI water was passed through the oFc20-modified membrane followed by 10 mL of 20 mM sodium phosphate (containing 500 mM NaCl, pH 7.4, Buffer C) for equilibration. Seven mL of 0.1 mg/mL Trastuzumab (Herceptin, unless otherwise noted) spiked in Buffer C was passed through the membrane at 0.5 mL/min, followed by passage of 10 mL of Buffer C and 10 mL of DI water at 1 mL/min. Trastuzumab concentrations in the load, permeate and wash solutions were determined by measuring the intrinsic tryptophan fluorescence (excitation at 280 nm, emission at 330 nm). For Protein A-modified membranes, Trastuzumab binding was performed similarly but without overnight circulation of Buffer B prior to binding.

Trastuzumab elution was performed under several different conditions. For Protein A-modified membranes, Pierce IgG elution buffer, 5% FA, and 0.1 M TCEP in 1 wt% SDS were investigated as eluents. For oFc20-modified membranes, we investigated elution

efficiency with Pierce IgG elution buffer, and 1, 3 or 5% FA as eluents. Three aliquots (0.5 mL) of each eluent were passed through fresh Trastuzumab-loaded membranes at 0.5 mL/min. The Trastuzumab concentrations in each eluate aliquot were determined by measuring intrinsic tryptophan fluorescence.

Digestion of Eluted mAb Using Pepsin-Containing Membranes.

0.3 mL of the first aliquot of Trastuzumab eluate from oFc20-modified membranes was mixed with 30 μL of 0.1 M TCEP and incubated at 75 °C for 15 min following a modified literature procedure.[43] The mixture was cooled to room temperature and diluted to 1 mL by adding 5% FA. A 0.64-cm diameter pepsin-functionalized membrane was immobilized into a miniaturized inline membrane holder (Upchurch Scientific A-424), and 100 μL of reduced and heat-denatured Trastuzumab eluate was pushed through the pepsin membrane at 1.8 mL/min using a syringe pump. The holder exposes a membrane area of 0.02 cm^2. After passing through the membrane, the digested aliquot was mixed with 100 μL of ACN to prevent in-solution digestion from any leached pepsin before evaporation to dryness using a SpeedVac concentrator. Finally, the digested product was reconstituted with 100 μL of a solution containing 4 vol% ACN and 0.1 vol% FA in water (Solution A). The digested products would not be returned to the original mAb sample.

Separation and Characterization of Digested mAb.

1 μL of reconstituted, digested Trastuzumab solution was injected into a Waters Nano Acquity UPLC system. The separation of peptides was performed using a Waters BEH C18 column (300 Å pore, 1.7 μm particle, 100 μm × 100 mm) with aqueous 0.1 % FA and ACN as mobile phases A (MPA) and B (MPB), respectively. The separation gradient went from 7 to 33% MPB in 20 min at a 0.9 μL/min flow rate with a 53 °C column temperature. Mass spectra were acquired using a ThermoFisher Q Exactive HF orbitrap, with a full MS1 spectrum with m/z from 385 to 1800. The MS2 spectra were obtained using a TOP17 data-dependent acquisition method, and higher-energy collisional dissociation (HCD) fragmentation applied.

The analysis of mAb glycan composition was performed manually by peptide mass fingerprinting as described previously.[44] The monoisotopic mass of a glycopeptide was matched in the MS1 spectrum, whereas the fragments of glycopeptide were searched in the MS2 spectra. The glycopeptide fragments can contain either an intact peptide backbone with part of the glycan or a partial peptide backbone.

Glycopeptide Degradation Analysis.

Trastuzumab stock solution was first buffer exchanged into DI water using a 3.5K MWCO dialysis device overnight. Dialyzed Trastuzumab was spiked into 3% FA to a final concentration of 0.2 mg/mL. Solutions were incubated at room temperature for 0 or 60 min before reduction and denaturation followed by the pepsin digestion described above. The glycan composition was monitored by comparing the relative peak areas of glycopeptides with different glycan forms with or without 60-min incubation in 3% FA.

Selective Enrichment of mAbs from Diluted Cell Culture Supernatant.

Chinese hamster ovary (CHO) cell lines are used extensively for mAb production due to their high yield and formation of desired PTMs. The reported titer of mAbs in CHO cells is as high as 10 g/L.[45] To obtain relevant cell culture supernatant host cell protein concentrations at 0.1 mg/mL mAb levels, blank (not transfected) ExpiCHO-S cell culture supernatant was spiked into different mAbs in Buffer C at a volume ratio of 1:100 (v/v). mAb solutions containing diluted cell culture supernatant were passed through oFc20-modified membranes for enrichment before mAbs were eluted then digested and analyzed by LC-MS. Figure 1 schematically shows the workflow for glycan analysis of mAbs from cell culture supernatant.

Transfected ExpiCHO-S cells expressing Ab3022 were cultured 7 days before supernatant was harvested and clarified. The concentration of Ab3022 in the supernatant was determined as 56 μg/mL using a Human IgG (total) ELISA with purified Ab3022 as standards.[39] To maintain a reasonable Ab3022 concentration in the feed solution, the Ab3022 supernatant was diluted 1:1 with Buffer C. 15 mL of the resulting solution was passed through oFc20-modified membranes for enrichment and subsequent glycan analysis.

Data Analysis.

To confirm the identity of Trastuzumab in eluate, the raw files acquired from the orbitrap mass spectrometer were mapped using PEAKS with 5 and 10 ppm as precursor and fragment error tolerance, respectively. The fragmentation method was set as HCD, with a semi-specific pepsin digestion (at least one proteolysis site at the C-terminus of F, L, Y or W),[46] and a maximum of 3 missed cleavages were applied to the search criteria.

The amino acid sequences of glycopeptides were obtained from processing raw data files with pGlyco3 software with the same criteria described above.[47] PEAKS and pGlyco3 search the raw data files based on both the MS1 and MS2 spectra. Peptides with low signals will not trigger fragmentation, thus pGlyco3 identifies only major glycopeptide sequences.

The monoisotopic m/z values of glycopeptides consisting of amino acid sequences identified with pGlyco3 and various glycans were searched in the MS1 spectrum manually using the Xcalibur browser. To confirm the identity of these glycopeptides, their MS2 spectra were also manually finger-printed based on the monoisotopic masses of their fragments. The area under the curve (AUC) of each glycosylated- or aglycosylated-peptide was used to determine the relative peak area, which is the AUC for a specific glycan (including all glycopeptides with this glycan and all of their charge states) divided by the sum of peak areas for all identified glycopeptides (including all charge states) and the aglycosylated peptide.

RESULTS AND DISCUSSION

The analytical procedure includes capture of mAbs in ligand-modified membranes or resins, elution of the captured mAbs with dilute formic acid, reduction, in-membrane peptic digestion, and determination of glycopeptide peak areas in the eluate digest. Membranes or resins containing either oFc20 peptide or Protein A specifically enrich mAbs to allow

analysis of the glycan compositions in a wide range of human IgG mAbs. This section first compares the mAb binding capacities of Protein A- and oFc20-modified membranes using Trastuzumab as a test case. Second, we optimize the elution conditions prior to digesting reduced mAb eluates during flow through a pepsin-containing membrane. Third, we assess the glycan compositions of digested antibodies using LC-MS/MS. Lastly, this work shows that the method applies to various Human IgG drug products, including biosimilars and different subclasses of human IgGs, and an in-house expressed human IgG1 antibody. These studies also compare analyses using tryptic and peptic digestion.

Evaluation of Binding and Elution of Trastuzumab in Ligand-Modified Membranes.

Previously, we reported immobilization capacities of 14 ± 1 mg of Protein A and 8 ± 1 mg of oFc20 per mL of membrane in 2-cm diameter glass-fiber membranes.[39] We evaluated the Trastuzumab binding capacities by passing 7 mL of 0.1 mg/mL Trastuzumab in Buffer C through the membranes. Figure 2A shows the Trastuzumab binding capacities, which we calculated using mass balances obtained with analyses of Trastuzumab in feed, permeate and wash solutions. oFc20-modified membranes show higher Trastuzumab binding, due to a higher number of accessible binding sites or greater affinity towards the Fc region of Human IgGs.

To analyze the glycan profiles of therapeutic mAbs, including detection of glycan proteoforms with low peak areas, we aim to elute as much mAb as possible from the membranes. Thus, we examined elution efficiencies of both Protein A- and oFc20-modified membranes using several eluents. Figures 2B–C show the elution efficiencies, which are the ratios of eluted to initially bound Trastuzumab. Elution occurred in 3 consecutive 0.5 mL aliquots. For Protein A-modified membranes, Pierce IgG elution buffer does not elute Trastuzumab effectively, whereas 5% FA can give ~ 40% elution recovery. Higher recoveries require a harsh elution condition, consisting of 0.1 M TCEP in 1 wt% SDS. The low elution efficiency with Protein A is unusual, as Protein A-containing resins show high elution efficiencies (see section S2 in the supporting information).

Similarly, Pierce IgG elution buffer shows a low elution efficiency in oFc20-modified membranes. However, 1% FA can elute ~ 75% of bound Trastuzumab. The elution efficiency increases with a higher concentration of FA, but there is no significant difference between using 3 or 5% FA. Thus, oFc20-modified membranes show advantages over Protein A-based membranes in terms of both binding capacity and elution efficiency. Below we use 3% FA and oFc20-modified membranes for mAb capture, elution, and glycan analysis.

Identification of Trastuzumab Glycans Using LC-MS/MS.

After elution, we reduced and denatured the Trastuzumab eluate by adding TCEP and heating at 75 °C for 15 min. Digestion then occurred in <5 min by passing the denatured eluate through a pepsin-containing membrane. The digested product was dried and reconstituted in Solution A before analysis by LC-MS/MS. To confirm the identity of Trastuzumab in the eluate, we performed peptide mapping using PEAKS software and achieved 100% amino acid sequence coverage for both light and heavy chains (see Figure S2 in the supporting information).

To identify the *glyco*peptides, the raw data file was searched using pGlyco3 software, which found only two glycopeptide amino acid sequences, YVDGVEVHNAKTKPREEQYN-STYRVVSVL (denoted as YVDG--) and GVEVGVEVHNA-KTKPREEQYNSTYRVVSVL (denoted as GVEV--). Typically, the AUC of a YVDG-- peptide is about twice the AUC of the GVEV-- peptide with the same glycan. Perhaps other glycopeptide sequences are present, but their low intensity did not trigger MS/MS fragmentation. Additionally, pGlyco3 only identified glycoforms with high peak areas: G0F, G1F, G2F, G0 and M5. YVDG-- and GVEV-- contain 3 and 2 missed cleavages, respectively. (We define possible missed cleavage sites as F, L, Y, and W.) Two of the missed cleavage sites are near the N300 glycosylation site, which may hinder digestion. Notably, the N-terminus of GVEV-- results from non-specific pepsin digestion. We examined 4 IgG1 antibodies (see below), and all of them showed the same sequences for glycopeptides, and other subclasses of antibodies show related peptides. Thus, despite the promiscuity of pepsin,[48] the digestion is reproducible.

Through manual searching of the mass spectra, we identified 11 major glycan forms in eluted Trastuzumab: G0F, G1F, G2F, G0, G1, G2, G0F-GN, G1F-GN, G0-GN, M5 and M6 (see Table S1 in the supporting information for their compositions). Figures S3A–D show the extracted ion chromatograms (XICs) of YVDG-- and GVEV-- glycopeptides with different glycan forms at a 5+ charge state. We also observed some of these glycopeptides at 4+ or 6+ charge states. Figure S3E is the XIC of a peptide, YVDGVEVHNAKTKPREEQYNST, with no glycan present at N300. The observed monoisotopic m/z values of these glycopeptides show good agreement with their theoretical values as shown in Figures S4A–E and Figures S5A–D. The glycan fragmentations in their MS2 spectra also match with the monoisotopic masses of their potential fragments as Figures S6A–E and S7A–D show. The fragmentation on the YVDG-- or GVEV-- peptide backbone further confirms the identities of these glycopeptides, see Figures S8A–B. Hence, both MS1 and MS2 spectra enable identification of the different glycan forms.

Glycan Relative Peak Areas in Eluted Trastuzumab.

To mimic mAb isolation from a fermentation broth, we spiked Trastuzumab into a 1:100 (v/v) diluted CHO cell culture supernatant with no transfection.[45] The Trastuzumab concentration was 0.1 mg/mL, which would correspond to 10 mg/mL in undiluted supernatant. This is a typical mAb titer in fermentation. The experimental procedures remain the same as described above. Using LC-MS/MS and label-free quantitation, we estimated the glycan relative peak areas in Trastuzumab eluted with 3% FA, reduced, and digested with pepsin. As Figure S9 shows, G0F and G1F are the two most abundant glycan forms in eluted Trastuzumab, and this result aligns with the reported Trastuzumab glycosylation profile.[49] G0F and G1F account for 46 ± 4 and 33 ± 2%, respectively, of the total glycosylation peak areas in our analysis. G2F, G0 and M5 each represent about 5% of the total peak area, and the relative peak areas of G1, G2, G0F-GN, G1F-GN, G0-GN and M6 are even lower. The aglycosylated proteoform relative peak area is only ~ 0.7%, suggesting that most of the Trastuzumab is glycosylated. We also analyzed Trastuzumab samples eluted with 5 or 1% FA, and the glycosylation profiles agree with those obtained using 3% FA (Figure S9).

From elution to reduction, digestion and finally resuspension, the eluted Trastuzumab is in an acidic environment for less than 1 hour. However, the structures of glycans and mAbs may degrade at low pH.[50, 51] To examine whether the glycans of eluted Trastuzumab are stable in 3% FA, we spiked a Trastuzumab solution (dialyzed against DI water) into 3% FA, and incubated samples at room temperature for 60 min prior to analysis by LC-MS/MS. As Figure S10A shows, the glycan compositions of Trastuzumab in 3% FA are similar with and without a 60-min incubation in 3% FA. This suggests that the glycan compositions will remain unchanged in the acidic environment of the eluate for at least 60 min. Figure S10B compares the ratio between the AUC of glycopeptides and the AUC of a reference non-glycosylated peptide. This ratio does not change with acid incubation for 60 min. Thus, the glycan composition should not change during purification and elution.

We also compared the glycosylation profile of eluted and peptic-digested Trastuzumab with a profile from a Trastuzumab standard (in DI water) that was denatured, alkylated, and digested with trypsin. We previously reported the procedure for in-membrane trypsin digestion and showed that glycosylation profiles are similar after in-membrane and in-solution digestion,[44] although in-membrane digestion is much faster. Figure 3 shows the Trastuzumab glycosylation profiles obtained using trypsin or pepsin digestion. Both in-membrane digestions give similar Trastuzumab glycosylation patterns and relative peak areas. These data imply that the proposed capture, elution, and pepsin digestion workflow accurately reflect relative Trastuzumab glycan profiles with negligible degradation, although we do see some small variations in the relative peak areas of the rarer glycans between dialyzed Trastuzumab analyzed after tryptic digestion (in Figure 3) and dialyzed Trastuzumab standards (in Figure S10A) processed with pepsin in-membrane digestion in the Trastuzumab degradation study.

The rate of pepsinolysis may depend on the composition of the neighboring glycan. To examine whether such a scenario affects relative peak areas, we analyzed Trastuzumab digests after 1, 2 or 4 passes though the pepsin membrane. Figure S11A indicates that additional passes through the membrane give fewer missed cleavages and, hence, more identified unique peptides. Similarly, pGlyco3 found a shorter glycopeptide sequence YVDGVEVHNAKTKPREEQYNSTY (YVDG'--) after the 4-pass digestion. However, the relative peak areas of the various glycopeptides from 4-pass digestion are similar to those from the 1- or 2-pass digestion (Figure S11B). Thus, using YVDG-- and GVEV-- glycopeptides to assess the glycosylation pattern is reasonable. The similarity of glycan patterns after tryptic and peptic digestion also suggests that incomplete digestion does not alter the observed glycan profiles (Figure 3). Our previous publications concluded that the assessment of N-glycan patterns is comparable after in-membrane and in-solution digestion.[44]

The in-membrane peptic digestion is rapid, and the acidic conditions allow direct digestion of the 3% FA eluate without the alkylation and desalting that are typically part of tryptic digestion. We examined whether the peptic digestion is also compatible with enrichment using a Protein A spin column. Figure S12 shows that enrichments in membranes and spin columns give similar results in terms of glycan analysis.

Glycosylation analysis of Trastuzumab from Different Batches and Its Biosimilars.

Next, we examined the glycosylation pattern of Trastuzumab from three different manufacturing lots. The analysis procedures are the same as described earlier, and the Trastuzumab was spiked into a 1:100 (v/v) diluted blank CHO culture supernatant at a concentration of 0.1 mg/mL. As Figure 4 shows, the overall glycosylation patterns from the three different batches are similar but show a few small statistically significant differences (unpaired T test). The relative peak areas of G0F, G1F, G0, G2 and M5 show statistically significant batch-to-batch difference, although the differences in the intensities of the rarer glycans are dubious. The relative peak areas of G0F are 42 ± 3, 46 ± 4 and 49 ± 2% in batches 1, 2 and 3, respectively, whereas the G1F relative peak areas are 34 ± 3, 33 ± 2 and 28.9 ± 0.5% in the three batches. Notably, batch 3 has the highest G0F peak area and the lowest G1F peak area. Similar differences in mAb glycosylation were observed before.[52, 53] Such analyses may provide important initial screening for mAb production and quality control. We should note that the antibodies were stored at −20 °C in their formulation buffers for several months prior to analysis, and such storage might cause small changes in glycosylation patterns.

We also investigated the glycosylation profiles of Trastuzumab biosimilars, Kanjinti and Ogivri. They have the same amino acid sequence and similar pharmacology profiles as the original Trastuzumab drug product Herceptin but might be manufactured in different methods. As glycosylation is a critical quality attribute for mAbs, and it can vary under different manufacturing conditions, we examined the glycosylation differences among these products. Figure S13 shows the glycosylation compositions of these three Trastuzumab products. The two main glycan forms of Trastuzumab, G0F and G1F both show similar relative peak areas across all three products. However, the relative peak areas of G2, G0F-GN, G1F-GN and M5 show significant product-to-product differences, although the magnitude of all these peak areas is small. Interestingly, Herceptin shows the highest degree of aglycosylation among all three products, but this only accounts for 0.7% of the total peak area.

Glycosylation Profiling of Various mAbs.

To demonstrate that our workflow is suitable for profiling glycan compositions of various mAbs, we analyzed two additional IgG1 mAbs, Rituximab and Cetuximab. Both of them contain the same Fc region as Trastuzumab, however, their glycan profiles might be different. As Figure S14 shows, the glycosylation patterns of Rituximab and Cetuximab are different from Trastuzumab. Although the relative peak areas of major glycan forms, G0F, G1F and G2F are similar among these three IgG1 mAbs, significant differences appeared in other glycan forms. Cetuximab shows the highest degree of high mannose glycan M5 compared to Trastuzumab and Rituximab. Goetze and Kanda reported that mAbs with high mannose glycans have decreased circulation half-life,[54, 55] but all of the mAbs have relatively low levels of these glycans.

Although IgG1 is the most common subclass of therapeutic mAbs, IgG2 and IgG4 are also employed when designing and screening antibodies. To investigate the suitability of our assay for analyzing IgG2 and IgG4 therapeutic mAbs, we also

analyzed Panitumumab and Nivolumab. Despite the different amino acid sequences of IgG2 and IgG4 compared to IgG1, the pepsin digestion showed similar peptides for all of the mAbs. The amino acid sequences of glycopeptides of Panitumumab after pepsin digestion are YVDGVEVHNAKTKPREEQFNS-TFRVVSVL (noted as YVDG2--) and GVEVHNAKTKP-REEQFNSTFRVVSVL (noted as GVEV2--), both consisting of a two amino acid difference compared to the glycopeptides of IgG1. Figures S15A–E show the XICs of these peptides with different glycans, as well as the XIC of an aglycosylated peptide containing the N294 site. For Nivolumab, the glycopeptides are one amino acid different from those in the IgG1 glycopeptides, and they are YVDGVEVHNAKTKPREEQFNSTYRVVSVL (noted as YVDG4--) and GVEVHNAKTKPREEQFNS-TYRVVSVL (noted as GVEV4--). Figures S16A–D show the XICs of these peptides with different glycans, as well as the XIC of an aglycosylated peptide containing the N289 site. As Figure 5 shows, the glycan compositions of Panitumumab and Nivolumab show significant differences relative to Trastuzumab. Panitumumab has similar relative peak areas of G0F and G1F compared to Trastuzumab, but lower relative peak areas of afucosylated glycans (G0, G1, G2, G0-GN). Additionally, the relative peak areas of high mannose glycans (M5 and M6) in Panitumumab are higher than in Trastuzumab. For Nivolumab, G0F is the most abundant glycan form, with a 60.7 ± 7.3% relative peak area. Accordingly, this mAb gave the lowest relative peak area of G1F among all mAbs analyzed (16.1 ± 2.7%). To our surprise, we did not find any G2, M5 and M6 glycan forms, potentially because of their low peak areas in Nivolumab. We also noticed the highest relative peak area of aglycosylated peptide in Nivolumab. This result aligns with a Nivolumab tryptic digest result (Figure S17).

Analysis of the Glycan Composition of Ab3022, An In-House Expressed IgG1 mAb.

Ab3022 targets the S1 domain of SARS-CoV or SARS-CoV-2 spike protein. To further challenge the robustness of our workflow, CHO cell culture supernatant containing 56 μg/mL Ab3022 was diluted 1:1 (v/v) with Buffer C prior to passing through oFc20-modified membranes for analysis. Figure 6 shows the glycan profile of Ab3022. G0F and G1F are the two most abundant glycan forms of Ab3022. Interestingly, we did not observe any afucosylated glycans, G0, G1, G2 and G0-GN. The relative peak areas of high mannose glycans, M5 and M6, are higher than other mAbs, and the degree of aglycosylation is also higher than in the other IgG1 mAbs we analyzed. The different pattern of glycosylation of Ab3022 might derive from the expression system. Although both Ab3022 and other IgG1 mAbs were expressed in CHO cells, their cell clones are different.

To address whether affinity enrichment is necessary in glycosylation profiling, we directly digested the Ab3022-containing cell culture supernatant to compare with our current approach. The total protein concentration of Ab3022-containing cell culture supernatant is 23 ± 6 mg/mL as assessed through protein precipitation, dialysis, and a Pierce 660 nm protein assay. The supernatant was diluted with DI water to 0.3 mg/mL total protein concentration before reduction, denaturation and digestion through the pepsin membrane following the same procedure described earlier. However, we did not find any YVDG-- or GVEV-- glycopeptides. Hence, affinity enrichment is crucial to the analysis of mAb glycosylation in cell culture supernatant.

Workflow Time Cost Breakdown, And Potential Improvements.

The described workflow comprises four main sections, binding, elution, digestion and LC-MS analysis. In the current format, the mAb enrichment takes 14 min, whereas washing with phosphate buffer and DI water takes 20 min. The elution of captured mAb requires 1 min, and reduction/denaturation of the mAb eluate takes 15 min. Rapid pepsin digestion occurs in only 4 min. Drying requires 15 min, and the LC-MS separation and analysis takes 48 min, including column washing and equilibration. In total, the time cost is under 2 hours. In conventional approaches, the PNGase or trypsin enzymatic reaction alone can be at least 2 hours. The use of analytical high-performance LC and multiple reaction monitoring mass spectrometry might shorten the time for analysis of each sample to ~5 min.[56–58] We also propose integrating affinity or protease membranes into spin columns or 96-well plates to reduce the time for enrichment and washing, and potential coupling with liquid handling robots for automation.

We can envision an in-flow method where fermentation broth is passed through a series of filters for clarification, binding, elution, digestion, and sent directly to LC-MS. This process could be automated with a series of pumps, streamlining the workflow and enhancing efficiency. With such improvements, the process may prove effective for monitoring the continuity of glycan proteoform expression during fermentation. Furthermore, such a method might be used for high-throughput screening of cell lines for antibody production, optimization of media components for specific glycosylation patterns, and determination of appropriate storage conditions for proteins.

CONCLUSION

This study demonstrates a workflow for quickly enriching and digesting therapeutic mAbs for glycosylation analysis. oFc20-modified affinity membranes are advantageous over Protein A-based membranes in terms of higher mAb binding capacity and elution recovery. Eluate digestion occurs in a pepsin-functionalized membrane in as little as 4 min, and elution with 3% FA and pepsin digestion avoid alkylation and desalting, simplifying the sample preparation. Nanoflow LC coupled with Orbitrap MS enables assessment of glycosylation patterns. This approach shows similar mAb glycan profiles to analyses after digestion with trypsin, and the assay is effective for many different mAbs, including biosimilars and IgG2 and IgG4 mAbs. Impressively, this method is suitable for harvested cell culture supernatant even with just 2-fold dilution with phosphate buffer. Future work may focus on integrating oFc20-modified membranes into spin columns or 96-well plate formats to further shorten processing time and give more customer-suitable devices.

Supplementary Material

Refer to Web version on PubMed Central for supplementary material.

ACKNOWLEDGMENT

We are grateful to the National Science Foundation (Grant IIP-2122540), the NSF IUCRC Center for Bioanalytical Metrology (1916601), and the National Institute Of General Medical Sciences of the National Institutes of Health (R01GM149786) for funding this work. The content does not necessarily represent the official views of the

National Institutes of Health. We thank Dr. William C. Boggess from the Mass Spectrometry & Proteomics Facility at the University of Notre Dame for his help with LC-MS instrument setup and data analysis. We also thank Hui Yin Tan, Adrianna Bickner, and Weikai Cao for conducting pilot studies for this project, and Dr. Christopher Welch of the Indiana Consortium for Analytical Science & Engineering for helpful discussions and editing. The CR3022 encoding plasmids were produced under HHSN272201400008C and obtained through BEI Resources, NIAID, NIH: Plasmid Set for Anti-SARS Coronavirus Human Monoclonal Antibody CR3022, NR-53260. The illustration figures were created with BioRender.com.

REFERENCES

(1). Jaffe GJ; Dick AD; Brézin AP; Nguyen QD; Thorne JE; Kestelyn P; Barisani-Asenbaur T; Franco P; Heiligenhaus A; Scales D; Chu DS; Camez A; Kwatra NV; Song AP; Kron M; Tari S; Schuler EB Adalimumab in Patients with Active Noninfectious Uveitis. N. Engl. J. Med. 2016, 375 (10), 932–943. DOI: 10.1056/NEJMoa1509852 [PubMed: 27602665]

(2). Levin MJ et al. Intramuscular AZD7442 (Tixagevimab-Cilgavimab) for Prevention of Covid-19. N. Engl. J. Med. 2022, 386 (23), 2188–2200. DOI: 10.1056/NEJMoa2116620 [PubMed: 35443106]

(3). Swain SM; Shastry M; Hamilton E Targeting HER2-Positive Breast Cancer: Advances and Future Directions. Nat. Rev. Drug Discov. 2023, 22 (2), 101–126. DOI: 10.1038/s41573-022-00579-0 [PubMed: 36344672]

(4). Alt N; Zhang TY; Motchnik P; Taticek R; Quarmby V; Schlothauer T; Beck H; Emrich T; Harris RJ Determination of Critical Quality Attributes for Monoclonal Antibodies Using Quality by Design Principles. Biologicals 2016, 44 (5), 291–305. DOI: 10.1016/j.biologicals.2016.06.005 [PubMed: 27461239]

(5). Majewska NI; Tejada ML; Betenbaugh MJ; Agarwal N N-Glycosylation of IgG and IgG-Like Recombinant Therapeutic Proteins: Why Is It Important and How Can We Control It? Annu. Rev. Chem. Biomol. Eng. 2020, 11, 311–338. DOI: 10.1146/annurev-chembioeng-102419-010001 [PubMed: 32176521]

(6). Sethuraman N; Stadheim TA Challenges in Therapeutic Glycoprotein Production. Curr. Opin. Biotechnol. 2006, 17 (4), 341–346. DOI: 10.1016/j.copbio.2006.06.010 [PubMed: 16828275]

(7). Smith LM; Kelleher NL Proteoforms as the Next Proteomics Currency. Science 2018, 359, 1106–1107. DOI: 10.1126/science.aat1884 [PubMed: 29590032]

(8). Li T; DiLillo DJ; Bournazos S; Giddens JP; Ravetch JV; Wang LX Modulating IgG Effector Function by Fc Glycan Engineering. Proc. Natl. Acad. Sci. U S A 2017, 114 (13), 3485–3490. DOI: 10.1073/pnas.1702173114 [PubMed: 28289219]

(9). Liu L Antibody Glycosylation and Its Impact on The Pharmacokinetics and Pharmacodynamics of Monoclonal Antibodies and Fc-Fusion Proteins. J. Pharm. Sci. 2015, 104 (6), 1866–1884. DOI: 10.1002/jps.24444 [PubMed: 25872915]

(10). Pereira NA; Chan KF; Lin PC; Song Z The “Less-Is-More” in Therapeutic Antibodies: Afucosylated Anti-Cancer Antibodies with Enhanced Antibody-Dependent Cellular Cytotoxicity. mAbs 2018, 10 (5), 693–711. DOI: 10.1080/19420862.2018.1466767 [PubMed: 29733746]

(11). Spadiut O; Capone S; Krainer F; Glieder A; Herwig C Microbials for The Production of Monoclonal Antibodies and Antibody Fragments. Trends Biotechnol. 2014, 32 (1), 54–60. DOI: 10.1016/j.tibtech.2013.10.002 [PubMed: 24183828]

(12). Hossler P Protein Glycosylation Control in Mammalian Cell Culture: Past Precedents and Contemporary Prospects. In Advances in Biochemical Engineering Biotechnology. Springer 2018, pp 187–219. DOI: 10.1007/10_2011_113

(13). Carillo S; Pérez-Robles R; Jakes C; Ribeiro da Silva M; Martin SM; Farrell A; Navas N; Bones J Comparing Different Domains of Analysis for the Characterization of N-Glycans on Monoclonal Antibodies. J. Pharm. Anal. 2020, 10 (1), 23–34. DOI: 10.1016/j.jpha.2019.11.008 [PubMed: 32123597]

(14). Kim Y; Li H; Choi J; Boo J; Jo H; Hyun JY; Shin I Glycosidase-Targeting Small Molecules for Biological and Therapeutic Applications. Chem. Soc. Rev. 2023, 52 (20), 7036–7070. DOI: 10.1039/d3cs00032j [PubMed: 37671645]

(15). Geng W; Jiang N; Qing G; Liu X; Wang L; Busscher H; Tian G; Sun T; Wang L; Montelongo Y; Janiak C; Zhang G; Yang X; Su B Click Reaction for Reversible Encapsulation of Single Yeast Cells. ACS Nano 2019, 13, 14459–14467. DOI: 10.1021/acsnano.9b08108 [PubMed: 31804798]

(16). Zhang T; Geng W; Huang Y; Wang F; Tian G; Yang X Specific Recognition to Create Nanofunctionalized Cells for Precise functions. Coordin. Chem. Rev. 2024, 498, 215471. DOI: 10.1016/j.ccr.2023.215471

(17). Zhu Z; Ramakrishnan B; Li J; Wang Y; Feng Y; Prabakaran P; Colantonio S; Dyba MA; Qasba PK; Dimitrov DS Site-Specific Antibody-Drug Conjugation Through an Engineered Glycotransferase and A Chemically Reactive Sugar. mAbs 2014, 6 (5), 1190–1200. DOI: 10.4161/mabs.29889 [PubMed: 25517304]

(18). Zhou Q; Stefano JE; Manning C; Kyazike J; Chen B; Gianolio DA; Park A; Busch M; Bird J; Zheng X; Simonds-Mannes H; Kim J; Gregory RC; Miller RJ; Brondyk WH; Dhal PK; Pan CK Site-Specific Antibody-Drug Conjugation Through Glycoengineering. Bioconjug. Chem. 2014, 25 (3), 510–520. DOI: 10.1021/bc400505q [PubMed: 24533768]

(19). Zauner G; Selman MH; Bondt A; Rombouts Y; Blank D; Deelder AM; Wuhrer M Glycoproteomic Analysis of Antibodies. Mol. Cell. Proteomics 2013, 12 (4), 856–865. DOI: 10.1074/mcp.R112.026005 [PubMed: 23325769]

(20). Li M; Feng Y; Ma M; Kapur A; Patankar M; Li L High-Throughput Quantitative Glycomics Enabled by 12-plex Isobaric Multiplex Labeling Reagents for Carbonyl-Containing Compound (SUGAR) Tags. J. Proteome Res. 2023, 22 (5), 1557–1563. DOI: 10.1021/acs.jproteome.2c00773 [PubMed: 36700627]

(21). Szigeti M; Bondar J; Gjerde D; Keresztessy Z; Szekrenyes A; Guttman A Rapid N-Glycan Release from Glycoproteins Using Immobilized PNGase F Microcolumns. J. Chromatogr. B Analyt. Technol. Biomed. Life Sci. 2016, 1032, 139–143. DOI: 10.1016/j.jchromb.2016.02.006

(22). Agilent. N-Glycan Analysis Tools and Reagents. https://www.agilent.com/cs/library/brochures/brochure-glycan-prep-prozyme-5994-1647EN-agilent.pdf (Accessed 2023-12-07)

(23). Leblanc Y; Faid V; Lauber MA; Wang Q; Bihoreau N; Chevreux G A Generic Method for Intact and Subunit Level Characterization of mAb Charge Variants by Native Mass Spectrometry. J. Chromatogr. B Analyt. Technol. Biomed. Life Sci. 2019, 1133, 121814. DOI: 10.1016/j.jchromb.2019.121814

(24). Dalpathado DS; Desaire H Glycopeptide Analysis by Mass Spectrometry. Analyst 2008, 133 (6), 731–738. DOI: 10.1039/b713816d [PubMed: 18493671]

(25). Wei J; Papanastasiou D; Kosmopoulou M; Smyrnakis A; Hong P; Tursumamat N; Klein JA; Xia C; Tang Y; Zaia J; Costello CE; Lin C De Novo Glycan Sequencing by Electronic Excitation Dissociation MS^2 Guided MS^3 Analysis on an Omnitrap-Orbitrap Hybrid Instrument. Chem. Sci. 2023, 14 (24), 6695–6704. DOI: 10.1039/d3sc00870c [PubMed: 37350811]

(26). Singh SK; Lee KH Characterization of Monoclonal Antibody Glycan Heterogeneity Using Hydrophilic Interaction Liquid Chromatography-Mass Spectrometry. Front. Bioeng. Biotechnol. 2021, 9, 805788. DOI: 10.3389/fbioe.2021.805788 [PubMed: 35087805]

(27). Shen X; Liang Z; Xu T; Yang Z; Wang Q; Chen D; Pham L; Du W; Sun L Investigating Native Capillary Zone Electrophoresis-Mass Spectrometry on A High-End Quadrupole-Time-of-Flight Mass Spectrometer for The Characterization of Monoclonal Antibodies. Int. J. Mass Spectrom. 2021, 462. DOI: 10.1016/j.ijms.2021.116541

(28). Leon IR; Schwammle V; Jensen ON; Sprenger RR Quantitative Assessment of In-Solution Digestion Efficiency Identifies Optimal Protocols for Unbiased Protein Analysis. Mol. Cell. Proteomics 2013, 12 (10), 2992–3005. DOI: 10.1074/mcp.M112.025585 [PubMed: 23792921]

(29). Yang X; Kim SM; Ruzanski R; Chen Y; Moses S; Ling WL; Li X; Wang SC; Li H; Ambrogelly A; Richardson D; Shameem M Ultrafast and High-Throughput N-glycan Analysis for Monoclonal Antibodies. mAbs 2016, 8 (4), 706–717. DOI: 10.1080/19420862.2016.1156828 [PubMed: 27082290]

(30). Osuofa J; Henn D; Zhou J; Forsyth A; Husson SM High-Capacity Multimodal Anion-Exchange Membranes for Polishing of Therapeutic Proteins. Biotechnol. Prog. 2021, 37 (3), e3129. DOI: 10.1002/btpr.3129 [PubMed: 33475239]

(31). Li Z; Gu Q; Coffman JL; Przybycien T; Zydney AL Continuous Precipitation for Monoclonal Antibody Capture Using Countercurrent Washing by Microfiltration. Biotechnol. Prog. 2019, 35 (6), e2886. DOI: 10.1002/btpr.2886 [PubMed: 31342667]

(32). Berwanger JD; Tan HY; Jokhadze G; Bruening ML Determination of the Serum Concentrations of the Monoclonal Antibodies Bevacizumab, Rituximab, and Panitumumab Using Porous Membranes Containing Immobilized Peptide Mimotopes. Anal. Chem. 2021, 93 (21), 7562–7570. DOI: 10.1021/acs.analchem.0c04903 [PubMed: 33999602]

(33). Tan HY; Yang J; Linnes JC; Welch CJ; Bruening ML Quantitation of Trastuzumab and An Antibody to SARS-CoV-2 in Minutes Using Affinity Membranes in 96-Well Plates. Anal. Chem. 2022, 94 (2), 884–891. DOI: 10.1021/acs.analchem.1c03654 [PubMed: 34982935]

(34). Yang L; Bui L; Hanjaya-Putra D; Bruening ML Membrane-Based Affinity Purification to Identify Target Proteins of a Small-Molecule Drug. Anal. Chem. 2020, 92 (17), 11912–11920. DOI: 10.1021/acs.analchem.0c02316 [PubMed: 32867494]

(35). Ning W; Bruening ML Rapid Protein Digestion and Purification with Membranes Attached to Pipet Tips. Anal. Chem. 2015, 87 (24), 11984–11989. DOI: 10.1021/acs.analchem.5b03679 [PubMed: 26629589]

(36). Bickner AN; Champion MM; Hummon AB; Bruening ML Electroblotting through a Tryptic Membrane for LC-MS/MS Analysis of Proteins Separated in Electrophoretic Gels. Analyst 2020, 145 (23), 7724–7735. DOI: 10.1039/d0an01380c [PubMed: 33000802]

(37). Ryan KA; Bruening ML Online Protein Digestion in Membranes Between Capillary Electrophoresis and Mass Spectrometry. Analyst 2023, 148 (7), 1611–1619. DOI: 10.1039/d3an00106g [PubMed: 36912593]

(38). Gong Y; Zhang L; Li J; Feng S; Deng H Development of the Double Cyclic Peptide Ligand for Antibody Purification and Protein Detection. Bioconjug. Chem. 2016, 27 (7), 1569–1573. DOI: 10.1021/acs.bioconjchem.6b00170 [PubMed: 27362542]

(39). Yang J; Ostafe R; Welch CJ; Verhalen B; Budyak IL; Bruening ML Rapid Quantitation of Various Therapeutic Monoclonal Antibodies Using Membranes with Fc-Specific Ligands. Anal. Chem. 2023, 95 (22), 8541–8551. DOI: 10.1021/acs.analchem.3c00531 [PubMed: 37216615]

(40). Saha K; Bender F; Gizeli E Comparative Study of IgG Binding to Proteins G and A: Nonequilibrium Kinetic and Binding Constant Determination with The Acoustic Waveguide Device. Anal. Chem. 2003, 75 (4), 835–842. DOI: 10.1021/ac0204911 [PubMed: 12622374]

(41). Tan YJ; Wang WH; Zheng Y; Dong J; Stefano G; Brandizzi F; Garavito RM; Reid GE; Bruening ML Limited Proteolysis via Millisecond Digestions in Protease-Modified Membranes. Anal. Chem. 2012, 84 (19), 8357–8363. DOI: 10.1021/ac3019153 [PubMed: 22950601]

(42). Liu W; Bennett AL; Ning W; Tan HY; Berwanger JD; Zeng X; Bruening ML Monoclonal Antibody Capture and Analysis Using Porous Membranes Containing Immobilized Peptide Mimotopes. Anal. Chem. 2018, 90 (20), 12161–12167. DOI: 10.1021/acs.analchem.8b03183 [PubMed: 30207156]

(43). Zhang H; Mcloughlin SM; Frausto SD; Tang H; Emmett MR; Marshall AG Simultaneous Reduction and Digestion of Proteins with Disulfide Bonds for Hydrogen/Deuterium Exchange Monitored by Mass Spectrometry. Anal. Chem. 2010, 82, 4, 1450–1454. DOI: 10.1021/ac902550n [PubMed: 20099838]

(44). Cao W; Bruening ML Analysis of Protein Glycosylation after Rapid Digestion Using Protease-Containing Membranes in Spin Columns. J. Am. Soc. Mass Spectrom. 2023, 34 (6), 1086–1095. DOI: 10.1021/jasms.3c00038 [PubMed: 37127550]

(45). Huang YM; Hu W; Rustandi E; Chang K; Yusuf-Makagiansar H; Ryll T Maximizing Productivity of CHO Cell-Based Fed-Batch Culture Using Chemically Defined Media Conditions and Typical Manufacturing Equipment. Biotechnol. Prog. 2010, 26 (5), 1400–1410. DOI: 10.1002/btpr.436 [PubMed: 20945494]

(46). Promega. Pepsin. https://www.promega.com/products/mass-spectrometry/proteases-and-surfactants/pepsin/?catNum=V1959 (Accessed 2023-12-07)

(47). Zeng WF; Cao WQ; Liu MQ; He SM; Yang PY Precise, Fast and Comprehensive Analysis of Intact Glycopeptides and Modified Glycans with pGlyco3. Nat. Methods 2021, 18 (12), 1515–1523. DOI: 10.1038/s41592-021-01306-0 [PubMed: 34824474]

(48). Hamuro Y; Coales SJ; Molnar KS; Tuske SJ; Morrow JA Specificity of Immobilized Porcine Pepsin in H/D Exchange Compatible Conditions. Rapid Commun. Mass Spectrom. 2008, 22 (7), 1041–1046. DOI: 10.1002/rcm.3467 [PubMed: 18327892]

(49). Giorgetti J; D'Atri V; Canonge J; Lechner A; Guillarme D; Colas O; Wagner-Rousset E; Beck A; Leize-Wagner E; Francois YN Monoclonal Antibody N-Glycosylation Profiling Using Capillary Electrophoresis - Mass Spectrometry: Assessment and Method Validation. Talanta 2018, 178, 530–537. DOI: 10.1016/j.talanta.2017.09.083 [PubMed: 29136858]

(50). Vlasak J; Ionescu R Fragmentation of Monoclonal Antibodies. mAbs 2011, 3 (3), 253–263. DOI: 10.4161/mabs.3.3.15608 [PubMed: 21487244]

(51). Nowak C; J KC; S MD; Katiyar A; Bhat R; Sun J; Ponniah G; Neill A; Mason B; Beck A; Liu H Forced Degradation of Recombinant Monoclonal Antibodies: A Practical Guide. mAbs 2017, 9 (8), 1217–1230. DOI: 10.1080/19420862.2017.1368602 [PubMed: 28853987]

(52). Yu YQA, J.; Gilar M Waters Corporation. Trastuzumab Glycan Batch-to-Batch Profiling using a UPLC/FLR/Mass Spectrometry Platform. https://www.waters.com/webassets/cms/library/docs/720003576en.pdf (Accessed 2023-12-07)

(53). Planinc A; Dejaegher B; Vander Heyden Y; Viaene J; Van Praet S; Rappez F; Van Antwerpen P; Delporte C Batch-to-batch N-glycosylation Study of Infliximab, Trastuzumab and Bevacizumab, and Stability Study of Bevacizumab. Eur. J. Hosp. Pharm. 2017, 24 (5), 286–292. DOI: 10.1136/ejhpharm-2016-001022 [PubMed: 31156959]

(54). Goetze AM; Liu YD; Zhang Z; Shah B; Lee E; Bondarenko PV; Flynn GC High-Mannose Glycans on The Fc Region of Therapeutic IgG Antibodies Increase Serum Clearance in Humans. Glycobiology 2011, 21 (7), 949–959. DOI: 10.1093/glycob/cwr027 [PubMed: 21421994]

(55). Kanda Y; Yamada T; Mori K; Okazaki A; Inoue M; Kitajima-Miyama K; Kuni-Kamochi R; Nakano R; Yano K; Kakita S; Shitara K; Satoh M Comparison of Biological Activity Among Nonfucosylated Therapeutic IgG1 Antibodies with Three Different N-Linked Fc Oligosaccharides: The High-Mannose, Hybrid, and Complex Types. Glycobiology 2007, 17 (1), 104–118. DOI: 10.1093/glycob/cwl057 [PubMed: 17012310]

(56). Yang N; Goonatilleke E; Park D; Song T; Fan G; Lebrilla CB Quantitation of Site-Specific Glycosylation in Manufactured Recombinant Monoclonal Antibody Drugs. Anal. Chem. 2016, 88, 14, 7091–7100. DOI: 10.1021/acs.analchem.6b00963 [PubMed: 27311011]

(57). Mu R; Huang Y; Bouquet J; Yuan J; Kubiak RJ; Ma E; Naser S; Mylott WR Jr.; Ismaiel OA; Wheeler AM; Burkart R; Cortes DF; Bruton J; Arends RH; Liang M; Rosenbaum AI Multiplex Hybrid Antigen-Capture LC-MRM Quantification in Sera and Nasal Lining Fluid of AZD7442, a SARS-CoV-2-Targeting Antibody Combination. Anal. Chem. 2022, 94, 14835–14845. DOI: 10.1021/acs.analchem.2c01320 [PubMed: 36269894]

(58). Huang Y; Del Nagro CJ; Balic K; Mylott WR Jr.; Ismaiel OA; Ma E; Faria M; Wheeler AM; Yuan M; Waldron MP; Peay MG; Cortes DF; Roskos L; Liang M; Rosenbaum AI Multifaceted Bioanalytical Methods for the Comprehensive Pharmacokinetic and Catabolic Assessment of MEDI3726, an Anti-Prostate-Specific Membrane Antigen Pyrrolobenzodiazepine Anti-body-Drug Conjugate. Anal. Chem. 2020, 92, 11135–11144. DOI: 10.1021/acs.analchem.0c01187 [PubMed: 32459957]

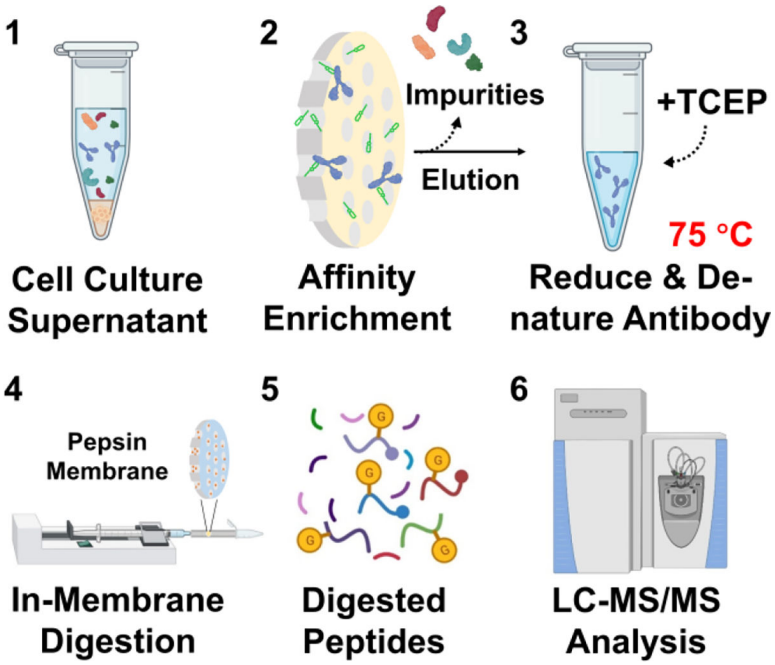

Figure 1.

Scheme of the experimental workflow for analyzing the glycan composition of mAbs in cell culture supernatant. The procedure includes selective enrichment of mAb from cell culture supernatant, elution of captured mAb, reduction and denaturation of eluted mAb, in-membrane digestion of eluate, drying (not shown) and analysis of peptides using LC-MS/MS.

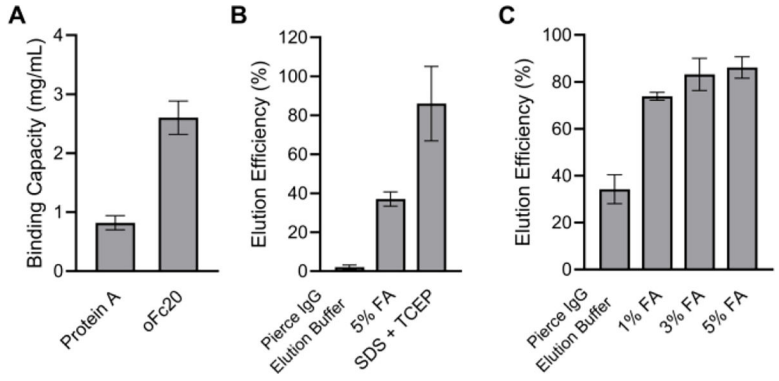

Figure 2.

Comparison of Trastuzumab binding and elution in Protein A- or oFc20-modified membranes. (A) Binding capacity of Protein A- or oFc20-modified membranes. The loading solution was 7 mL of 0.1 mg/mL Trastuzumab in Buffer C. (B, C) Efficiency of the elution of captured Trastuzumab in (B) Protein A- or (C) oFc20-modified membranes using different eluents. Error bars show the standard deviations from experiments with three different membranes.

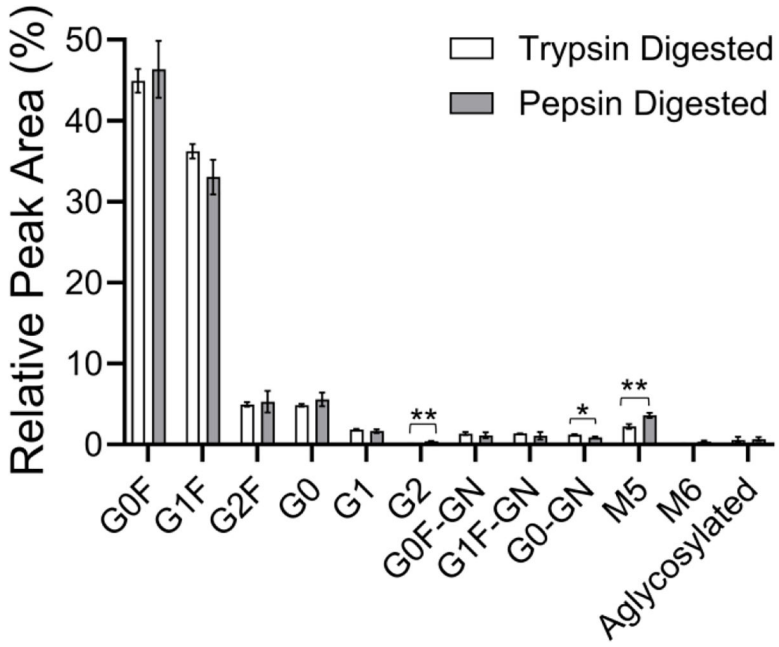

Figure 3.

Glycan relative MS1 peak areas for Trastuzumab digested with different proteases. The white columns are results of a Trastuzumab standard (in DI water) digested through trypsin in-membrane proteolysis. We observed two tryptic glycopeptides EEQYNSTYR and TKPREEQYNSTYR with 3+ and 4+ charge states. Grey columns represent Trastuzumab in the first eluate aliquot from an oFc20 membrane and processing with pepsin in-membrane digestion. The error bars are standard deviations of analyses of three digestion replicates either from the same dialyzed Trastuzumab standard in DI water or the first eluate aliquots from three different membranes. One and two *'s denote a significant difference at $p < 0.05$ or 0.01, respectively. The experimental section defines the relative peak area.

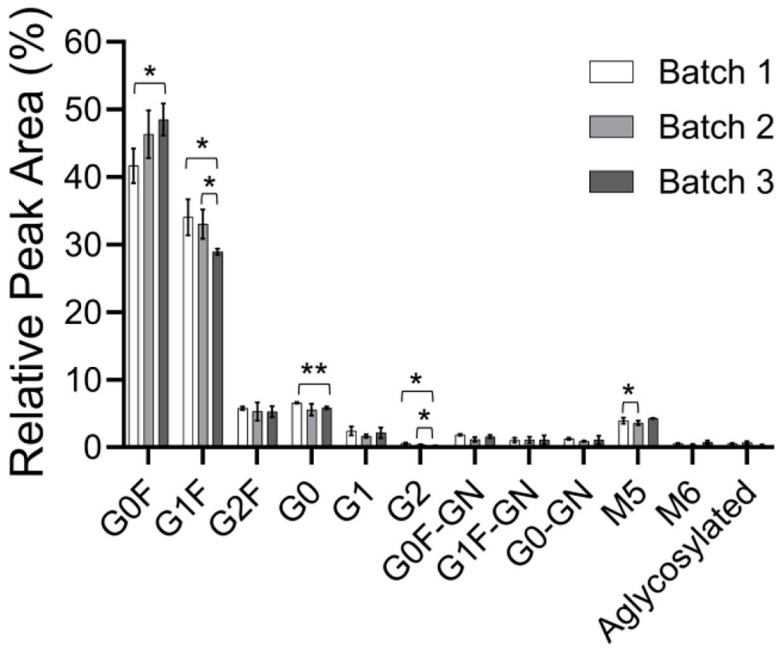

Figure 4.

Glycan compositions of Trastuzumab from three different manufacturing batches. Batch 2 is the Trastuzumab used for all Trastuzumab-related experiments here unless otherwise noted. * is $p < 0.05$, whereas ** is $p < 0.01$ in an unpaired T test. Error bars represent the standard deviations of analyses of the first eluate aliquot from three different membranes. The experimental section defines the relative peak area.

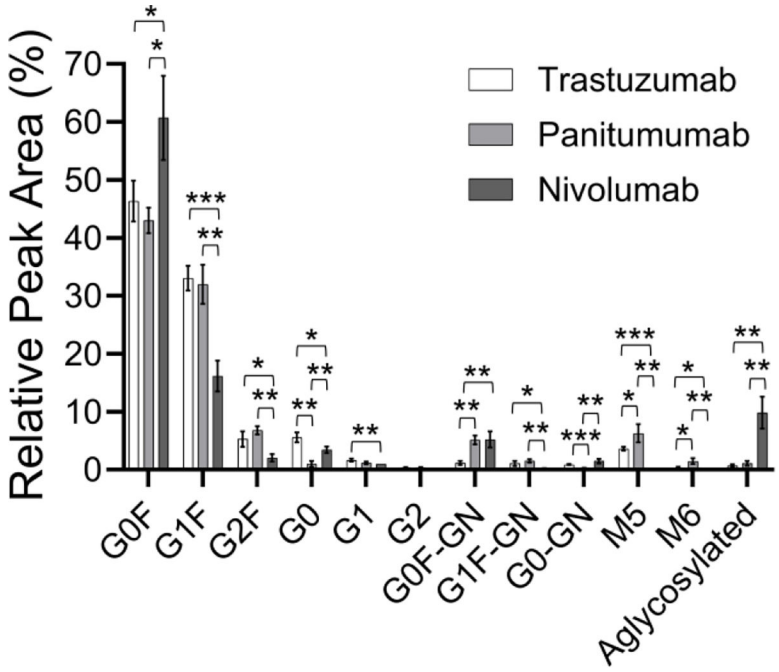

Figure 5.

Glycan compositions of three different subclasses of human IgGs. Trastuzumab is IgG1, whereas Panitumumab is IgG2 and Nivolumab is IgG4. The Trastuzumab result is the same as Batch 2 in Figure 4. Error bars represent the standard deviations of analyses of the first eluate aliquots from three different membranes. *** is $p < 0.001$ in unpaired T test. The experimental section defines the relative peak area.

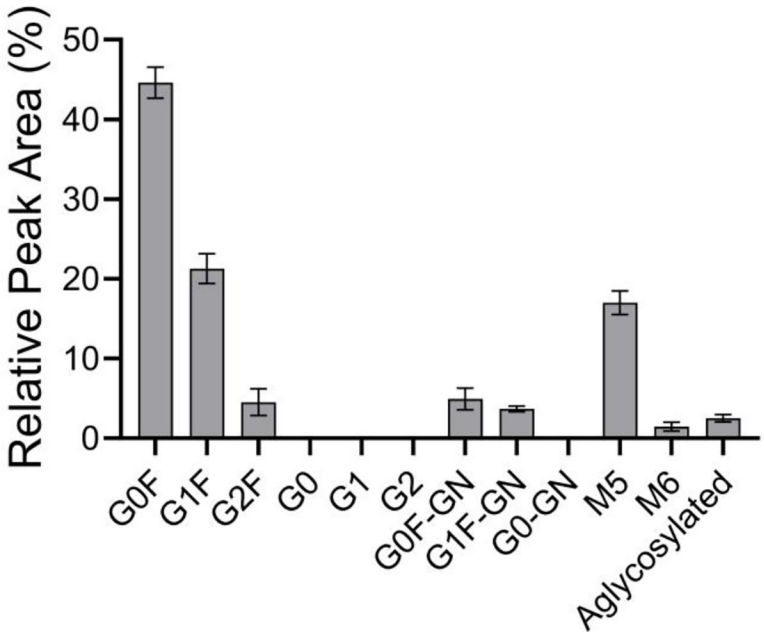

Figure 6.

Glycan composition of Ab3022, an in-house expressed human IgG1 antibody from ExpiCHO-S cells. The cells were cultured 7 days before harvest. The supernatant was clarified, and filter sterilized prior to analysis. Error bars are the standard deviations of measurements of replicate first eluate aliquots from three different membranes. The experimental section defines the relative peak area.